Partial Discharge Simulation and Detection in 750V DC XLPE Cables

C. B. Soh, C. K. Liew, S. Y. Cao, K. J. Tseng
Engineering Cluster, Singapore Institute of Technology 10 Dover Drive, Singapore (138683), Singapore

Pearl M. Z. Low, W. L. Woo
Newcastle University, SIT Building at Nanyang Polytechnic
127A Ang Mo Kio Avenue 8, #05-01
Singapore (567739), Singapore

Abstract— **This paper identifies and explores the different methodologies in detection of voids and signs of corrosion in the 750V DC XLPE cable insulation that causes partial discharge (PD), as well as analyzing its transient behaviour using MATLAB simulation. MATLAB software is used to study the partial discharge behaviour and their voltage waveforms with respect to the magnetic field. This allows better understanding of the occurrence of partial discharges and methods that can be used to predict future cable failures. Based on the Partial Discharge behaviour simulated by software and correlation with experimental results from Non-Destructive thermographic imaging of intentional generated defects in XLPE cables, it allows identification of voids and potential corroded cable. The work allows early detection of flaws, preventing potential cable failure and provide timely maintenance.**

Keywords— Partial Discharge, Thermography, Electrical Insulation, Electrical Tree

I. INTRODUCTION

Singapore Mass Rapid Transit (SMRT) was incorporated in 1987 and served more than 1.6 million passengers daily with 53 stations in the North-South and East-West line. The main power supply to the SMRT is stepped down and converted to 750V DC for the SMRT DC traction system. The XLPE cables which are 40mm in diameter are used to transmit the power from the substation to the third rail system. The third rail provides electrical traction power to the train and it is housed in insulating brackets alongside the running rails. The locomotive have metal collector shoes which are in contact with the third rail during operation. The XLPE insulated cables are the preferred choice for SMRT due to the cross-linking effect, which provides stability in elevated temperatures and has a low dielectric loss factor as compared to other thermoplastic materials. Hence, the good electrical and mechanical properties of XLPE insulated cables have made it applicable in high voltage industries [1].

Despite its advantages, the humid and hot environmental conditions the cable is subjected to during operation especially in the tunnel can have a great impact on the cable insulation performance. Minerals seepage from the soil and coastal sea water into tunnel can give rise to corrosion of the XLPE cables with time. The alteration in applied current with varying locomotive load leads to greater electrical stress which further weakens its insulation strength [2]. The combination of electrical potential in the cables with ionic chlorides and nitride impurity seepage caused electrochemical reaction in cables. This leads to internal discharge (or partial discharge) in cavity of the XLPE cables. Partial discharge (PD) is a phenomenon which occurs when there is an electrical discharge within a localized area as stated in IEC 60270 [3]. These internal arcs promote the breakdown of insulation, forming electrical trees [4,5]. Once the electrical tree has threaded sufficiently deep, it will exposed the copper conductor to the environment, resulting in a cable failure and risk of current leakage to the tunnel platform [6].

As Partial Discharge is one of the main causes of cable failures and it occurs at very high frequencies which accelerates the deterioration of the performance of the cable insulation. Therefore, it is crucial to detect PDs before it reaches the final stages of cable failure. In this work, PDs using capacitive load are modelled and observed at the Measuring Instrument (MI) with a specific voltage applied at 'V_S'. This is then correlated with thermal heat distribution using thermal imaging technique.

II. SIMULATION MODEL

Based on the cross-section of the SMRT XLPE Cable as shown in Fig 1a, there are two layers of insulation, PVC Outer Sheath and the XLPE insulation of 2mm thickness each. By using MATLAB Simulink software to model the cable, the magnetic field intensity and the voltage stress experienced by the cable can be simulated. Fig. 1b shows a simplified illustration of electrical tree growth within the cable insulation from the interface of XLPE layer with PVC insulation to the external surface.

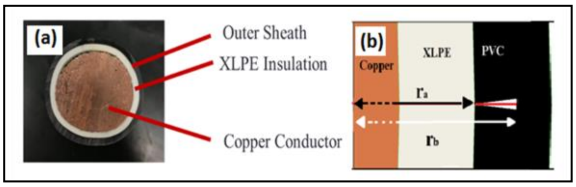

Fig. 1. (a) Cross-section of XLPE Cable (b) Tree Root Growth Model with 1.0mm in length within the PVC Insulation.

The tree growth will affects the magnetic field intensity across the cable. A PD Capacitive Model using MATLAB Simulink software was generated to model electrical tree root growth under the SMRT operating conditions. The length of a tree defect will affects the value of r_a and r_b (as shown in Fig. 1(b)) used for the MATLAB Simulation. The capacitance of the insulation and the tree defect can be calculated using the formulas as followed. The capacitance of the void within the insulation is given by

$$C_{void} = \frac{\theta_{void}\varepsilon_0\varepsilon_{air}l_{void}K_{cf}}{r_v\left(\ln\frac{r_b}{r_a}\right)}, \quad (1)$$

where the symbols within the formulas stated above are explained in Table 1. The dimensions of r_b and r_a are as illustrated in Fig 1b. K_{cf} is known as the correction factor of the cavity enclosed within the material and it is a dimensionless factor.

$$K_{cf} = \frac{3\varepsilon_r}{1 + 2\varepsilon_r} \quad (2)$$

The capacitance of the insulation enclosing the cavity is calculated using the following expression [7]:

$$C_{a+b} = \frac{\theta_{void}\varepsilon_0\varepsilon_{ins}l_{void}K_{cf}}{\left(\ln\frac{r_b}{r_a}\right)} \quad (3)$$

The capacitance of the remaining insulation across the cable is given by

$$C_{XLPE} = \frac{(2\pi - \theta_{void})\varepsilon_0\varepsilon_{ins}l_{void}K_{cf}}{\left(\ln\frac{r_b}{r_a}\right)} \quad (4)$$

The value of the capacitances determined from the equations above will be used for the simulation by MATLAB Simulink.

TABLE I
UNITS FOR CAPACITANCE PARAMETERS

Symbol	Representation	Constants
θ	Degrees	
ε_r	Relative dielectric constant	PVC, ε_r = 7 [13] XLPE, ε_r =2.25 [14]
ε_0	dielectric constant of air	8.854 × 10^{-12} F/m
l	Length	
r_a	Inner radius	
r_b	Outer radius	
r_v	Radius of the centroid of the void with reference to origin	

In the PD simulation model as shown in Fig. 2, 'V_S' is the high voltage source and R_{cond} represents the impedance within the copper conductor itself. 'C_k' is the coupling capacitor to to minimize the impedance for PD impulses to flow. Thus, 'C_k' has higher impedance of 1000µF as compared to the other capacitances. 'C_m' is a high voltage measuring capacitor required for a standard PD Experiment.

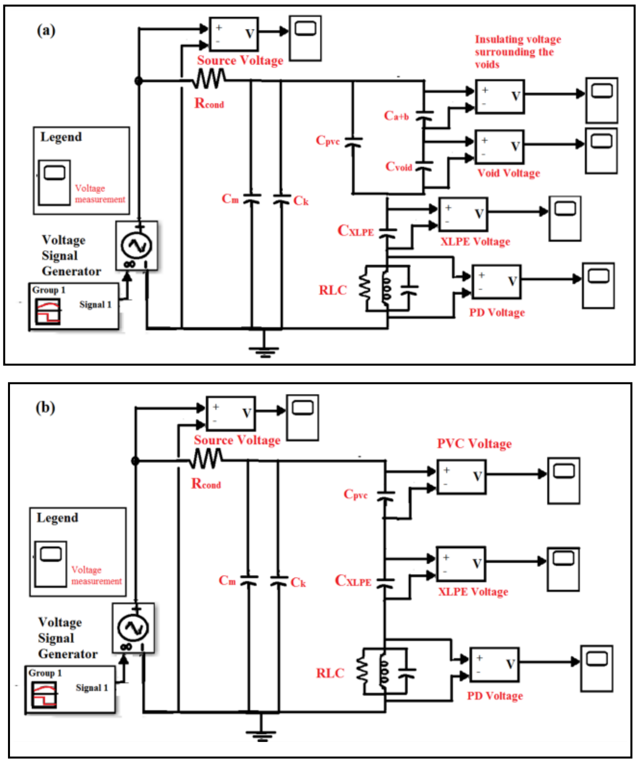

Fig. 2. Schematic Diagram of the Capacitive PD Model for (a) damaged (faulty) and (b) precinct Cable.

The standard value for 'C_m' is 1000pF. 'C_t' is the capacitance of the test object inclusive with a cavity embedded within the insulation capacitance. The 'RLC' branch represents the values of the PD detection device based on the standard PD Experiment. For our simulation, we follow the standard value for 'R', 'L' and 'C' as 50Ω, 0.63mH and 0.47µF respectively [8].

The MATLAB Simulink software is modelled after the tree root defect of 0.5mm in length. This test will compare a conventional cable with the damaged cable and record down its corresponding PD waveforms. The voltage source waveform used is set at 750V with a 10kV square pulse having a period of 1µs to mimic fast transient pulse typical for partial discharge. The PD pulse waveform between a normal cable and the faulty cable taken from the MI of the above equivalent circuits as shown in Fig. 2. (a) and (b) for a damaged (faulty) cable and conventional (normal) cable respectively across the RLC branch. The resultant PD waveform is as shown in Fig. 3. The results show that a higher PD voltage is detected and there is significant ripple effect before the signals dies off.

For a damaged (faulty) cable experiencing an abrupt voltage spike, it will cause voltage stress on the insulation. The voltage waveforms as shown in Fig. 3. is taken from the insulation scopes in Fig 2. (b) for the damage cable. The comparison between the voltage stresses at the PVC and the XLPE

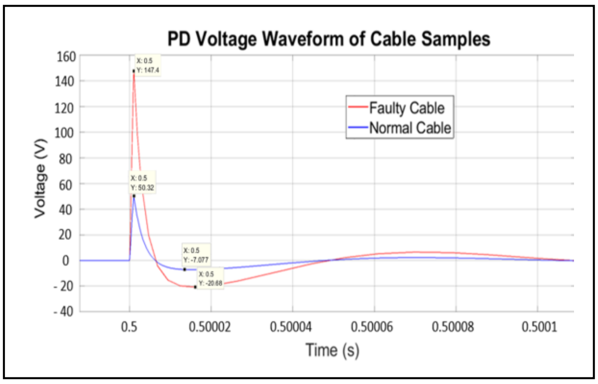

Fig. 3. PD Voltage Waveform between Normal and Faulty (damaged) Cable taken across the RLC cricuit

insulation is as shown in Fig. 4. The higher voltage measured for PVC as compared to XLPE is due to the higher dielectric constant of PVC insulation as compared to the XLPE insulation constant. The voltage stress for each region, namely the cavity, the insulation enclosing the cavity and the rest of the undamaged insulation are as shown in Fig. 4. The voltage waveforms are taken from the cavity and insulation scopes in Fig. 2b for a damaged cable.

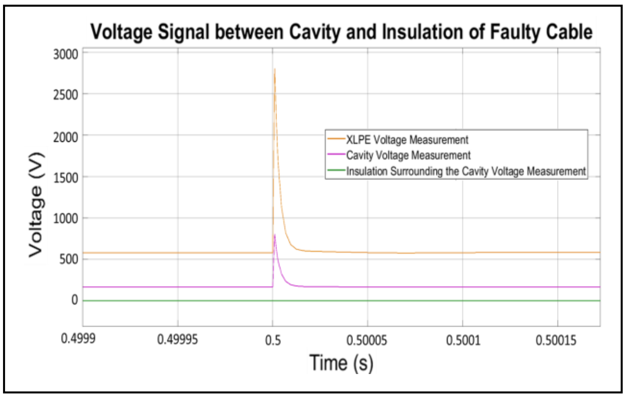

Fig. 4. PD Voltage Signal between Cavity and Insulation of Faulty Cable.

The Partial Discharge voltage signal for the faulty cable with treeing is as observed in Fig 4. A much higher voltage signal of ~2.7 kV is detected at the XLPE cable. On the otherhand, the cavity voltage which is made up of air with low dielectric constant has a PD voltage measured as 750V while the insulation surrounding the cavity has a PD voltage of close to zero as the PVC insulation around the void is short-circuited. This is due to the dielectric strengths of the cavity and the insulation. Since the dielectric strength of the XLPE insulation is 2.25 and air is 1, the change of dielectric strength and its calculated capacitances are based on Eqn 1 and Eqn 4. With lower dielectric strength, its overall calculated capacitance is much lower. Since reactance of a capacitive load is $X_c=1/j\omega C$, the impedance of the cavity increases as the capacitance decreases [10]. This causes higher impedance within the cavity and subsequently increase its voltage stress, as $V_c=I_c X_c$

III. EXPERIMENTAL DETAILS

Heat is one of the few detectable signs to alert maintenance engineers that there are signs of corrosion or PD phenomenon within the cable. The XLPE cable is trimmed into two cable samples and each sample was tested for signs of corrosion using passive thermographic imaging [9]. Fig. 5. shows the cables with holes drilled to reach the copper conductor. Cable A was the control specimen of the experiment with no corrosion process being done to it while Cable B went through the corrosion process for a period of 5 days by soaking in acetic acid and left to be oxidized. The cables were placed in a current driver bench unit, transmitting 1000A through the cables for a minute. To study the heat distribution of the copper conductor within and its insulation, holes were created within the samples at uniform intervals and the heat distribution were plotted.

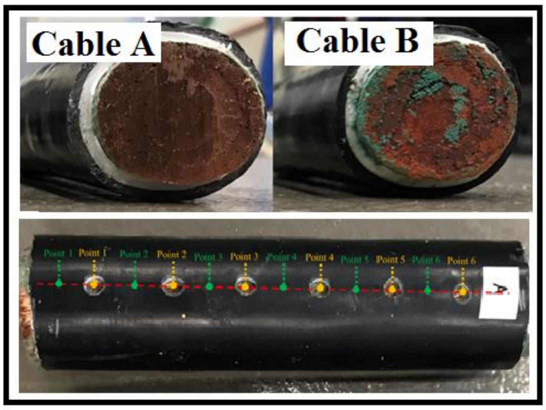

Fig. 5. Cable Samples for Corrosion Test using Thermography Imaging with holes created at uniform intervals.

For each sample, six holes were created and were labeled from Point 1 to Point 6 as shown in yellow, whereas the intervals the heat was measured at the insulation were also labeled Point 1 to Point 6 in green. The temperature across these points will be plotted in a graph for a clearer depiction of the heat distribution across both samples.

IV. EXPERIEMENTAL DETAILS

The thermographic imaging equipment uses a FLIR X6540sc infrared thermal camera with built-in software to display heat signatures of the test objects and the current driver bench unit powered by a Magnaflux P-1500 is used to transmit 1000A through the cables for this test. The current was transmitted for a minute, allowing heat to be produced by the cable during power transmission. The thermography results for both cable samples are shown in Fig. 6.

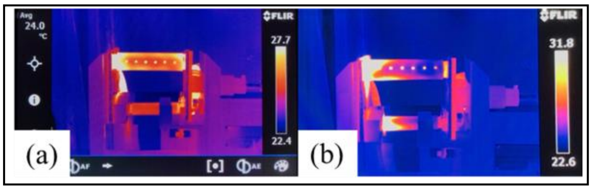

Fig. 6. Thermographs of (a) undamaged and (b) corroded cable samples.

Based on the thermography images in Fig. 6. above, the heat distribution across the undamaged cable was uniformly distributed and the heat distribution across the corroded cable were poorly distributed. Based on the results from the corroded cable and the undamaged cable, the heat distribution along the points as marked out in Fig. 5. are plotted in the graphs as shown in Fig 7(a) and (b).

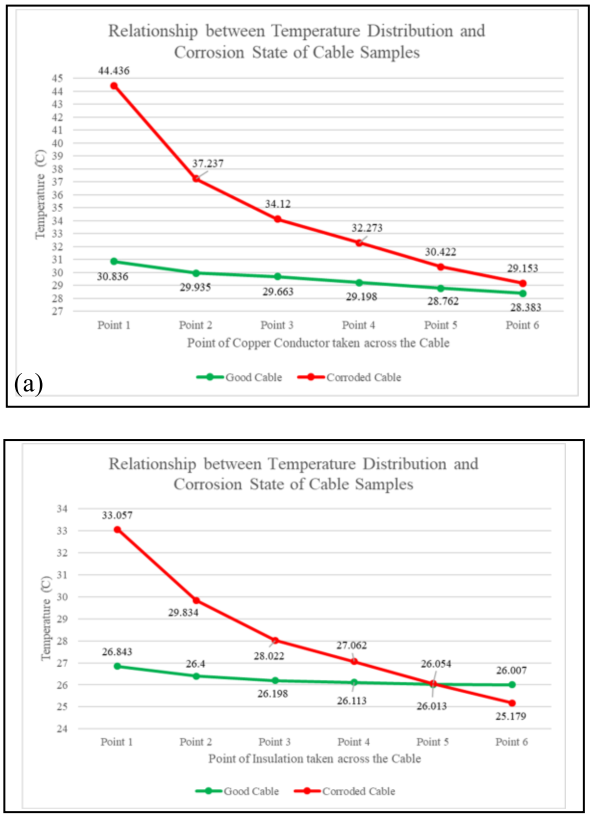

Fig 7(a) Heat Distribution of the Copper Conductor and (b) the Insulation.

The heat distribution characteristics for both the insulation and copper conductor are similar to one another. Observing the line graphs above, the highest temperature deviation (ΔT) from the average for the corroded cable is approximately 28.4% within the copper conductor and 17.22% for the cable insulation across Point 1 to Point 6. As for the cable in pristine condition, the ΔT within the copper conductor is approximately 4.66% and 2.21% for the cable insulation across Point 1 to Point 6. Therefore, insulation aging, corrosion of the internal copper conductors with subsequent water seepage which leads to PD phenomenon in the worst scenario can be prevented if thermal imaging is done to detect abnormal temperature difference along an existing operating cable. With higher temperature range as compared to a normal cable, there is power loss within the cable transmission, dissipated as heat to be detected by the thermography camera.

V. Conclusion

By investing on fault detection system, it can allow the early detection of PD phenomenon within the high DC voltage XLPE cable and potential system breakdown in the future. At later stages of PD phenomenon, further degradation of the XLPE cable will lead to cable failure. By inspecting the state of corrosion, engineers are able to gauge the lifespan of the cable and schedule for an asset replacement.

With the research of PD behaviour using software simulation, the main factors that contribute to PD phenomenon can be minimized. The main factors are voids within the cable insulation and the age of the cable. Voids within the cable insulation promotes high electrical stress that will cause accelerated cable degradation. With old cables, the resistance and dielectric strength of the insulation will wear out. Thermal testing was also found to be an effective non-contact inspection approach in detecting cable corrosion while reducing maintenance downtime. The current study for this project allows a better insight into PD behaviour and innovating different inspection methods that can detect early signs of cable degradation.

References

[1] "IEEE Guide for Specifying and Seldcting Power, Control and Special purpose cable petroleum and chemical plants", IEEE Standards 1242TM-2016

[2] X. Chen, X. Yang and X. Cao, "Nonlinear time series analysis of partial discharges in electrical trees of XLPE cable insulation samples - IEEE Journals & Magazine", (2014).

[3] "High voltage test techniques-Partial Discharge measurement", IEC 60270, (2000).

[4] Y. Zhang, Y. Zhou, L. Zhang, Z. Zhou, Q. Nie, "Electrical Trees and Their Growth in Silicone Rubber at Various Voltage Frequencies", Energies, 11, p327 (2018)

[5] M. H. Ahmad, N. Bashir, H. Ahmad, A. A. Abd Jamil, A. A. Suleiman, "An overview of Electrical Tree Growth in Solid Insulating Material with Emphasis of influencing factors, Mathematical Models and Tree Suppression" Telkomnika Indo. J. Elect. Eng. V12, 8 p5827-5846 (2014)

[6] M. A. Sandidzadeh, A. Shafipour, "Controlling and simulation of stray currents in DC railways by considering the effects of collection mats", INTECH, Infrastructure Design, Signalling and Security in Railway, Chp9, pg 225-254 (2012),

[7] S. Gopinath, K. Sathiyasekar, "Simulation of Partial discharges in solid dielectric material: A study on PD magnitudes to the parallel and perpendicular axis of a cylindrical cavity", Int. J. Eng. & Tech.v6, pp1786-1792, (2014).

[8] L. A. Utracki, J. A. Jukes, "Dielectric studies of polyvinyl chlorides"J. Vinyl & Additive Technology v6, pp85-94, Wiley (1984)..

[9] "Electromagnetic field | physics", Encyclopedia Britannica, 2017.

[10] M. Fard, A. Reid, D. Hepburn and M. Farrag, "Partial discharge behavior under HVDC superimposed with transients", 2016 51st International Universities Power Engineering Conference (UPEC), 2016.